# Assessment of Simulations of Snow Depth in the Qinghai-Tibetan Plateau Using CMIP5 Multi-Models

Authors: Wei, Zhigang, and Dong, Wenjie

Source: Arctic, Antarctic, and Alpine Research, 47(4) : 611-625

Published By: Institute of Arctic and Alpine Research (INSTAAR), University of Colorado

URL: https://doi.org/10.1657/AAAR0014-050

*Arctic, Antarctic, and Alpine Research, Vol. 47, No. 4, 2015, pp. 611–625*

# Assessment of simulations of snow depth in the Qinghai-Tibetan Plateau using CMIP5 multi-models

*Zhigang Wei*[1,2,3] *and Wenjie Dong*[1,2]

[1]State Key Laboratory of Earth Surface Processes and Resource Ecology, Beijing Normal University, No. 19, Xinjiekouwai Street, Haidian District , Beijing 100875, China
[2]Future Earth Research Institute, Beijing Normal University, No. 18, Jinfeng Road, Tangjiawan, Zhuhai, Guangdong 519087, China
[3]Corresponding author: wzg@bnu.edu.cn

## Abstract

The depths of snow in the Qinghai-Tibetan Plateau simulated by 19 phase five of the Coupled Model Inter-Comparison Project (CMIP5) models are assessed in comparison with the observation ones from passive microwave satellite remote-sensing (PMSR) and 72 weather stations. The annual regional mean snow depths (ARMSDs) from 1851 to 2005 indicate decreases for most of the models but slight increases for CMCC-CM, FGOALS-g2, and CanESM2. The simulated ARMSD anomalies vary from –10 cm to 20 cm, and the amplitudes exhibit obvious decreases over the recent 50 years. In the period from 1986 to 2005, the spatial distributions of the annual mean snow depth (AMSD) simulated by MRI-CGCM3, CCSM4, CESM1-BGC, CESM1-CAM5, and CESM1-WACCM are quite similar to those from the PMSR observations. But the maximum and mean AMSD values simulated by all 19 models are much larger than those observed by PMSR. The inter-annual variation of snow, which occurs primarily in the Middle and East Tibetan Plateau, is simulated relatively well by inmcm4. From 1960 to 2005, the ARMSDs simulated by most of the models show decreases but are increasing according to actual observations. Only five models produce positive trends that agree with the observations. According to the selected indices, the CCSM4, MIROC5, MRI-CGCM3, and FGOALS-g2 models are selected as relatively good models for predicting the plateau snow, and the 21st century changes in the snow climate in the Qinghai-Tibetan Plateau are projected using these four models.

DOI: http://dx.doi.org/10.1657/AAAR0014-050

## Introduction

The presence of snow increases the surface albedo and soil moisture and thermally isolates the atmosphere from the ground, thereby affecting the energy balance of the earth-atmosphere system. By acting as a seasonal reservoir of water, snow also strongly modifies the hydrological cycle (Räisänen and Eklund, 2012). The response of snow variation is highly sensitive to climate change. The snow is considered to be a potentially sensitive indicator of climate change, and due to feedback processes, changes in the spatial distribution/extent of land-based snow may play important roles in determining the direction and magnitude of climate changes across the globe (Clark and Serreze, 2000; Derksen et al., 1997). The Qinghai-Tibetan Plateau is the world's highest and largest plateau. It covers an area of more than 2 million km$^2$ at an average height of 4000 m above sea level, which represents one-fourth of the land area of China, and is one of the most important regions of snow in the Eurasian Continent. The thermal effect of snow can directly reach the middle of the troposphere. By acting as an elevated thermal source as well as a topographic barrier, the Qinghai-Tibetan Plateau has a profound impact on both local weather and global climate (Moore, 2012). At the end of the 19th century, Blanford (1884) first revealed that the winter-spring snow in the Himalayas had a negative correlation with the succeeding summer monsoon rainfall over India. Thereafter, many researchers have proved using data analysis and numerical simulation that the Qinghai-Tibetan Plateau snow plays significant roles in climatic variations in Asia (Guo and Wang, 1986; Wei et al., 1998; Chen and Song, 2000; Qian et al., 2003; Zhang et al., 2012). The snow anomalies over the Qinghai-Tibetan Plateau change the soil moisture and the surface temperature through the snowmelt process at first, and subsequently alter heat, moisture, and radiation fluxes from the surface to the atmosphere. Therefore, changes in the Qinghai-Tibetan Plateau snow have become a research focus in the past 20 years.

Most components of the cryosphere display decaying trends in the past century, especially over the latest 50 years (Qin and Xiao, 2009). The IPCC 5th Assessment report (Stocker et al., 2013) points out the following: the cryosphere is a natural integrator of climate variability and provides some of the most visible signatures of climate change. Snow is one important component of the cryosphere. Snow cover extent has decreased in the northern hemisphere, especially in spring (very high confidence). Most investigations show that the snow is decreasing with global warming in the northern hemisphere. Monotonic trend analysis of northern hemisphere snow cover extent over the period 1972–2006 with the Mann-Kendall test reveals significant declines during spring over North America and Eurasia, with lesser declines during winter and some increases in fall (Stephen and Ross, 2007). Northern hemisphere March snow-covered area shows a substantial decrease since about 1970, and this decrease corresponds to an increase in mean winter northern hemisphere temperature (Gregory and David, 2010). The spring snow cover has undergone significant reductions over the past 90 years, and the rate of decrease has accelerated over the past 40 years in the northern hemisphere. The observed northern hemisphere spring snow cover extent has decreased by about $0.8 \times 106$ km$^2$ per decade since 1970 (Brown and Robinson, 2011).

However, as first noted by Groisman et al. (1993) and more recently by Räisänen (2007), the snow cover response to global warming could vary with latitude and elevation, with a potential for increased accumulation in high latitudes and high elevations, where


1523-0430/02 $7.00

increases in precipitation are sufficient to offset reductions in the length of the accumulation season. An analysis of the trends in snow cover duration from the National Oceanic and Atmospheric Administration (NOAA) data during the 1966–2007 period shows that the largest decreases are concentrated in a zone where seasonal mean air temperatures fell in the range of –5 to +5 ºC and extended around the mid-latitudinal coastal margins of the continents (Brown and Mote, 2009). The snow depth and snow cover days in the Qinghai-Tibetan Plateau exhibit increasing trends in the past few decades (Wei et al., 2002; Qin et al., 2006; Zhang et al., 2008; Wang et al., 2009; Kang et al., 2010; You et al., 2011; Ma et al., 2011; Han et al., 2011), but these trends are unlike those in the northern hemisphere. However, the investigation also shows that the snow cover in winter and spring appears to undergo a slowly increasing trend in the past 40 years of the 20th century (Gao et al., 2003) and a decreasing trend from approximately 1998 to 2010 in the Qinghai-Tibetan Plateau (Wei et al., 2002; Zhang et al., 2008; Wang et al., 2009; Ma et al., 2011). For centurial time scale, some paleoclimate data show a decreasing trend of snow accumulation since the 1850s that is related to large-scale changes in the atmospheric circulation in the Qinghai-Tibetan Plateau (Moore, 2012, 2013).

The climate will continue to warm in future with the increase in greenhouse gas emissions, and how the snow conditions will change is a matter of great concern. Projections of the snow changes generally have been implemented using global climate models or high-resolution regional climate models. To understand the projections, it is important to assess the snow simulations in past years in comparison with observation data. Previous studies on snow assessment have concentrated on North America, North Europe, or the northern hemisphere. Most models underestimate mean winter North American snow cover extent (Frei and Gong, 2005). All of North America except parts of northern Canada shows a decrease in snow cover over the 21st century (Peacock, 2012). The water equivalent of the snowpack in northern Europe will decrease under the Special Report on Emissions Scenarios A1B scenario in 21st century (Räisänen and Eklund, 2012). The global model BCC_CSM1.1 can reproduce the spatial distribution of snow cover day and snow water equivalent over China and estimate snow cover changes over China under representative concentration pathway (RCP) scenarios (Ji and Kang, 2013). Immerzeel et al. (2013) have used results from the latest ensemble of climate models in combination with a high-resolution glacio-hydrological model to assess the hydrological impact of climate change on two climatically contrasting watersheds in the Greater Himalaya. The results show that the largest uncertainty in future runoff is a result of variations in projected precipitation between climate models and glaciers will recede but net glacier melt runoff is on a rising limb at least until 2050.

At present, phase five of the Coupled Model Inter-Comparison Project (CMIP5) has been conducted via a new set of coordinated climate model experiments using a new generation of Global Climate Models (GCMs) (Taylor et al., 2012). Brutel-Vuilmet et al. (2013) have compared the 20th century seasonal northern hemisphere land snow cover as simulated by available CMIP5 model output to observations, and the results show that the models reproduce the observed snow cover extent very well on average but the significant trend toward a reduced spring snow cover extent over the 1979–2005 period is underestimated. Zhu and Dong (2013) have pointed out that the CMIP5 coupled models can catch the main distribution characteristics of the observed northern hemisphere March-April snow cover but overestimate the mean snow cover in complex terrain area such as Qinghai-Tibet Plateau.

In summary, the Qinghai-Tibetan Plateau snow plays a significant role on both local weather and global climate. Snow cover extent has decreased in the whole of northern hemisphere and the CMIP5 coupled models can reproduce these characteristics. In the Qinghai-Tibetan Plateau, the snow has a decreasing trend since the 1850s; but the snow cover in winter and spring appears to undergo a slowly increasing trend in the past 40 years of the 20th century and a decreasing trend since the end of the 20th century. The CMIP5 simulations of mean snow cover are higher than the observation one in Qinghai-Tibetan Plateau. But, the simulations of the CMIP5 models to geographical distributions, trend, and inter-decadal variations of snow depth aren't evaluated in detail in the Qinghai-Tibetan Plateau in previous studies. The main purpose of this paper is to evaluate the ability of CMIP5 models to model these characteristics of the snow depths in the Qinghai-Tibetan Plateau in past decades, in order to identify systematic model biases and models that agree best with observations. The 21st century changes in the snow climate in the Qinghai-Tibetan Plateau will also be projected using CMIP5 models.

## Data and Methods

Snow depth (Snd) output data sets are obtained from 19 CMIP5 models (Table 1) through the Program for Climate Model Diagnosis and Intercomparison (PCMDI) Gateway website (http://pcmdi9.llnl.gov/esgf-web-fe) operated by the Earth System Grid Federation (ESGF). The core simulations within the suite of the CMIP5 long-term experiments include an AMIP run, a coupled control run, and a "historical" run forced by the observed atmospheric composition changes (reflecting both anthropogenic and natural sources) and included a time-evolving land cover for the first time. The historical experiment covers much of the industrial period, and its purpose is to evaluate a model's performance against the present climate and observed climate change, provide initial conditions for future scenario experiments, and evaluate the human impact on past climate (Taylor et al., 2012). The historical experiment data sets (only historical_r1i1p1) from 1850 to 2005 are used to assess the climate model performances with respect to simulating the present snow climate. The postfix r1i1p1 is the ensemble member used to distinguish among members of an ensemble typically generated by initializing a set of runs with different, but equally realistic, initial conditions. CMIP5 historical runs initialized from different times of a control run, for example, would be identified by "r1," "r2," "r3," etc. The postfix i1 is the "initialization method indicator" to distinguish the initial conditions. The postfix p1 is the "perturbed physics" number to distinguish perturbed physics ensemble. The postfix r1i1p1 means a first realization of the first version of the perturbed physics model.

Two types of snow data are available, which are taken from satellites and weather stations. The satellite data also can be divided into two types. One is the visible light snow data, and the other is the microwave snow data. The snow data from the microwave remote sensors can more accurately reflect the variation of the snow on the Tibetan Plateau (Wei et al., 2002). The scanning multichannel microwave radiometer (SMMR) is an imaging five-frequency radiometer (6, 10,18, 21, and 37 GHz) flown on the Nimbus-7 Earth satellites launched in 1978. The Special Sensor Microwave/Imager (SSM/I) sensors on the U.S. Defense Meteorological Satellite Program satellite collect data for four frequencies: 19, 22, 37, and 85 GHz. The original Chang algorithm (Chang et al.,1987) for passive remote sensing

**TABLE 1**

**Information for the 19 CMIP5 models.**

| Modeling Center (or Group) | Institute ID | Model name | Model number | Global snow grid resolution (nlon × nlat) |
|---|---|---|---|---|
| Beijing Climate Center, China Meteorological Administration | BCC | bcc-csm1-1 | 1 | 128 × 64 |
| Canadian Centre for Climate Modelling and Analysis | CCCMA | CanESM2 | 2 | 128 × 64 |
| National Center for Atmospheric Research | NCAR | CCSM4 | 3 | 288 × 192 |
| Community Earth System Model Contributors | NSF-DOE-NCAR | CESM1-BGC | 4 | 288 × 192 |
| | | CESM1-CAM5 | 5 | 288 × 192 |
| | | CESM1-WACCM | 6 | 144 × 96 |
| Centro Euro-Mediterraneo per I Cambiamenti Climatici | CMCC | CMCC-CM | 7 | 480 × 240 |
| LASG, Institute of Atmospheric Physics, Chinese Academy of Sciences and CESS,Tsinghua University | LASG-CESS | FGOALS-g2 | 8 | 128 × 60 |
| First Institute of Oceanography, SOA, China | FIO | FIO-ESM | 9 | 128 × 64 |
| NASA Goddard Institute for Space Studies | NASA GISS | GISS-E2-H | 10 | 144 × 90 |
| | | GISS-E2-R | 11 | 144 × 90 |
| | | GISS-E2-R-CC | 12 | 144 × 90 |
| Institute for Numerical Mathematics | INM | inmcm4 | 13 | 180 × 120 |
| Japan Agency for Marine-Earth Science and Technology, Atmosphere and Ocean Research Institute (University of Tokyo), and National Institute for Environmental Studies | MIROC | MIROC-ESM | 14 | 128 × 64 |
| | | MIROC-ESM-CHEM | 15 | 128 × 64 |
| Atmosphere and Ocean Research Institute (University of Tokyo), National Institute for Environmental Studies, and Japan Agency for Marine-Earth Science and Technology | MIROC | MIROC5 | 16 | 256 × 128 |
| Meteorological Research Institute | MRI | MRI-CGCM3 | 17 | 320 × 160 |
| Norwegian Climate Centre | NCC | NorESM1-M | 18 | 144 × 96 |
| | | NorESM1-ME | 19 | 144 × 96 |

of snow depth underestimates the snow depth at the beginning of the snow season and overestimates it at the end. By using SMMR and SSM/I remote-sensing data with the global cylindrical equal-area projection and snow-depth data recorded at the China national meteorological stations, the Chang algorithm is modified and validated using meteorological observation data considering the influences from vegetation, wet snow, precipitation, cold desert, and frozen ground; the modified algorithm is dynamically adjusted based on the seasonal variation of grain size and snow density; the algorithm suitable for snow-depth retrieval in China covering Qinghai-Tibetan Plateau is done and the gridded daily snow depths are derived (Che et al., 2008). Based on the observed snow data from 74 weather stations, Wang et al. (2013) have analyzed the accuracy of the snow data derived by Che et al. (2008) in Qinghai-Tibetan Plateau. The results show that there is a good consistency between the

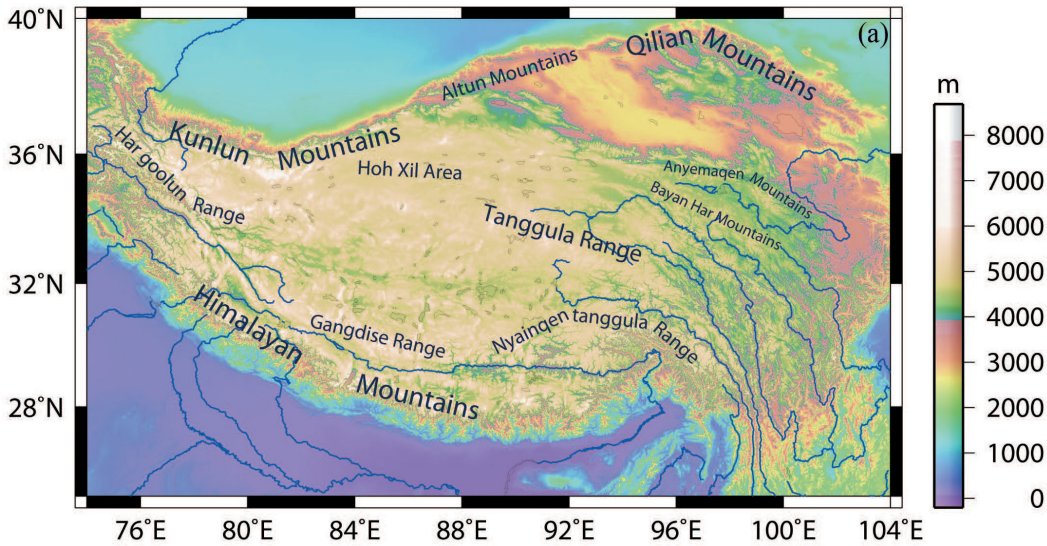


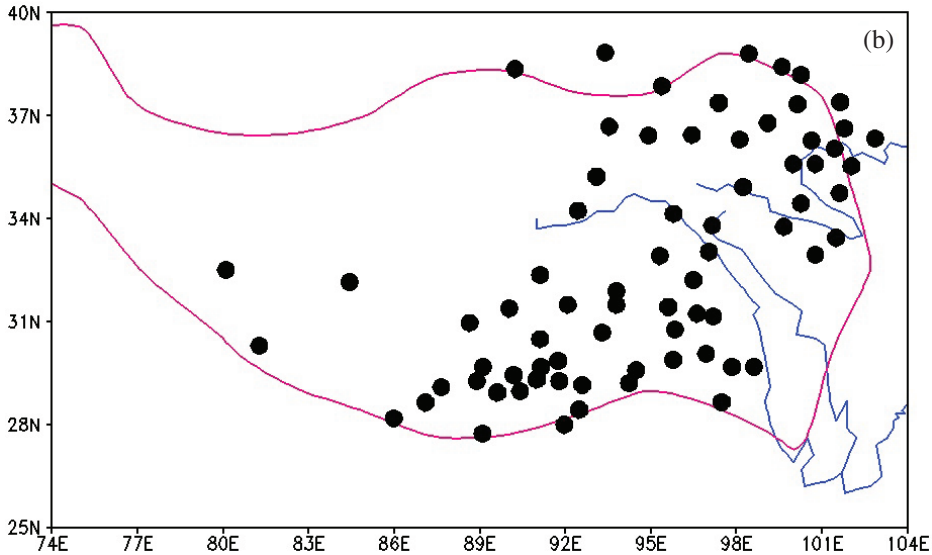


**FIGURE 1. (a) Topography and regional mountain ranges and (b) domain and location of the 72 weather stations (black circles) in the Qinghai-Tibetan Plateau. (The red curve shows the outline of the Plateau above the 3000-m sea level, and the blue curves indicate the Yellow River and the Yangzi River).**

passive microwave remote sensing data and the observed data in significant seasonal characteristics and annual variations of snow cover. The high seasonal snow cover regions from the passive microwave remote sensing data are consistent to one from the observed data. The snow data from the microwave remote sensors can more accurately reflect the spatial characteristics. Hence, in this study, the gridded daily snow depths derived by Che et al. (2008) from passive microwave satellite remote-sensing (PMSR) data in China with a resolution of 0.25° latitude × 0.25° longitude from 1985 to 2005 are selected to compare the spatial distribution with the model results. These data sets are obtained from the Environmental and Ecological Science Data Center for West China (website: http://westdc.westgis.ac.cn) at the Chinese Academy of Sciences.

In this paper, the Qinghai-Tibetan Plateau is located from 74°E to 104°E and from 25°N to 40°N. Figure 1 shows the domain, topography, and regional mountain ranges in the Qinghai-Tibetan Plateau. This domain shows the traditional Qinghai-Tibetan Plateau that does not include the Tianshan Range in the Xinjiang Autonomous Region and Hindu Kush Mountains to Chinese west border. The sets of the Tibetan Plateau snow consist of the mean of all grid values in the domain. The snow data from the microwave remote sensors are not suitable for analysis of inter-decadal variation because it appears too recently and the data set is too short. Hence, the daily snow depths in the Qinghai-Tibetan Plateau at the 72 weather stations (Fig. 1, part b) from 1959 to 2005 are chosen for comparison of the inter-annual and inter-decadal snow variation with the model results. The missing values usually exist in the meteorological records due to some causes. The temporal continuousness of the 72 station observations have been analyzed by Wei et al. (2002). The results show that if the station data for which the mean missing value times are greater than two per month aren't used to the annual mean snow depth, the station numbers of the usable winter-spring data will be less than 15 from 1953 to 1956, 18 in 1957, 36 in 1960, 50 in 1966, and about 70 in the recent years; the four sets of plateau

snow including (1) mean of the normalized snow depth sets, (2) normalized ratio of the station number that snow depth anomalies are positive and the total station number, (3) mean of the normalized snow day sets, (4) normalized ratio of the station number that snow day anomalies are positive and the total station number are analyzed; the inter-annual and inter-decadal variations of these sets are basically consistent. The plateau mean snow depths between the station data and the passive microwave remote sensing data have a good consistency in significant seasonal characteristics and annual variations (Wang et al., 2013). The missing values of snow depth exist almost every year. In this paper, if the mean missing value times are greater than two per month at any station, the data of the station will not be used to compute the annual mean snow depth.

By analysis of the snow data from weather stations in the Qinghai-Tibetan Plateau, generally, snow exists from October to May, with a certain amount of snow present in September and June and nearly no snow present in July and August (Wei et al., 2002). We assume that a snow year begins in August and ends in July. For example, 1851 indicates the snow year from 1 August 1850 to 31 July 1851, and the remainder may be deduced by analogy. The Snd averaged from 1 August to 31 July is treated as the annual mean snow depth (AMSD). Although very little snow occurs in July and August at weather stations, some snow exists always in the alpine region of the plateau. So, July and August are included in the annual mean. The AMSD averaged from 74°E to 104°E and from 25°N to 40°N is interpreted as the annual regional mean snow depth (ARMSD) in the Tibetan Plateau. All data have been interpolated onto a common 1° × 1° grid to compute the spatial correlation coefficient between the simulations and observations.

## Results

### *THE ANNUAL REGIONAL MEAN SNOW DEPTH AND ITS ANOMALIES FROM 1851 TO 2005*

Figure 2 shows the time series of the ARMSD values and their anomalies in the Qinghai-Tibetan Plateau from 1851 to 2005. The mean ARMSD values are approximately 5 cm for FIO-ESM and CMCC-CM but approximately 50 cm for GISS-E2-H. The black curve in Fig. 2, part a, denotes the observed ARMSD averaged using the data from 72 weather stations from 1960 to 2005. The stations are few in the alpine region and the mean snow depths from 72 weather stations are very much lower than those from models. Here, the mean observation snow depth from 72 weather stations is chosen for comparison of the inter-annual and inter-decadal snow variation with the model results and replotted at the top right corner in Figure 2, part a. Table 2 shows the trend and correlation coefficients between the observations and simulations. In the 155 years from 1851 to 2005, the ARMSDs (see Fig. 2, part a, and TR1 in Table 2) show decreases for most of the models, and the largest trend coefficient is –0.0917 cm $a^{-1}$ for GISS-E2-H; but the ARMSDs show rather small increases for CMCC-CM, FGOALS-g2, and CanESM2, with trend coefficients of 0.0006, 0.0018, and 0.0034 cm $a^{-1}$, respectively.

The simulated ARMSD anomalies (see Fig. 2, part b) vary from –10 cm to 20 cm, and the amplitudes show obvious decreases over the most recent 50 years. The black curve in Fig. 2, part b, denotes the observed ARMSD anomalies averaged using the data from 72 weather stations from 1960 to 2005; its amplitude is much smaller than that of the simulations because different samples are used to average the simulations and the observation. Su et al. (2013) evaluated precipitation and temperature over the eastern Tibetan Plateau by comparing the outputs of 24 CMIP5 GCMs with ground observations for the period 1961–2005. The results suggest that the majority of the models have cold biases, with a mean underestimation of 1.1–2.5 °C for the months December–May, and less than 1 °C for June–October. For precipitation, the simulations of all models overestimate the observations in climatological annual means by 62.0%–183.0%. A reason there is more snow in the simulation is that the simulated temperature is too cold and the simulated precipitation is too much over Qinghai-Tibetan Plateau. The cold temperature biases and the positive precipitation biases both might contribute to excessive simulated snow depths over the Qinghai-Tibetan Plateau.

The temporal variation of the simulated snow from 1960 to 2005 will be investigated in detail later in this paper.

### *SPATIAL DISTRIBUTION AND VARIATION CHARACTERISTICS OF THE SIMULATED SNOW DURING THE PERIOD 1986–2005*

The snow depths derived from PMSR data (Che et al. 2008) are selected only to compare the actual spatial distribution with the modeled results. Figure 3 shows the geographical distributions of the mean AMSD observed by PMSR and simulated by the 19 CMIP5 models from 1986 to 2005 in the Qinghai-Tibetan Plateau. The observation values from PMSR are much smaller than those of the CMIP5 simulations. According to the AMSDs from the PMSR observation, two maximum snow regions exist in the Qinghai-Tibetan Plateau. One region ranges from the Har goolun Range in the West Plateau to the Himalayan Mountains in the South Plateau, and the other reaches from the Nyainqentanggula Range to the East Tanggula Range and the Bayan har Range in the East Plateau. These locations are consistent with the previous research results (Li, 1995; Wei and Lu, 1995;Wei et al., 2002). The snow is relatively more plentiful in the Qilian Mountains and Hoh Xil Area. The two maximum snow regions are correctly simulated by most of the models. The spatial distributions of the mean simulated AMSD from MRI-CGCM3, CCSM4, CESM1-BGC, CESM1-CAM5, and CESM1-WACCM, whose spatial correlation coefficients between the simulated and the observation AMSD (R1 in Table 2) are larger than 0.65, are quite similar to those from the PMSR observations. Certain models (including the two Japanese models MIROC-ESM-CHEM and MIROC-ESM and three Chinese models FIO-ESM, FGOALS-g2, and bcc-csm1-1 show that only one maximum AMSD center occurs in the West Tibetan Plateau. These results are not consistent with the PMSR observations. Although the maximum regions are simulated by the three models from NASA Goddard Institute for Space Studies (GISS), the AMSDs and its spatial variations are much larger than those of the PMSR observation. In addition, the maximum AMSD values simulated by all 19 models are 5–15 times greater than those observed by PMSR. Hence, the normalized standard deviation values (modeled standard deviation divided by measured standard deviation) are quite large.

Figure 4 shows the geographical distributions of the mean simulated standard deviations of AMSD for the PMSR observations and the 19 CMIP5 models in the period from 1986 to 2005 in the Qinghai-Tibetan Plateau. The observation shows that the maximum value region occurs in the origin area of three rivers in

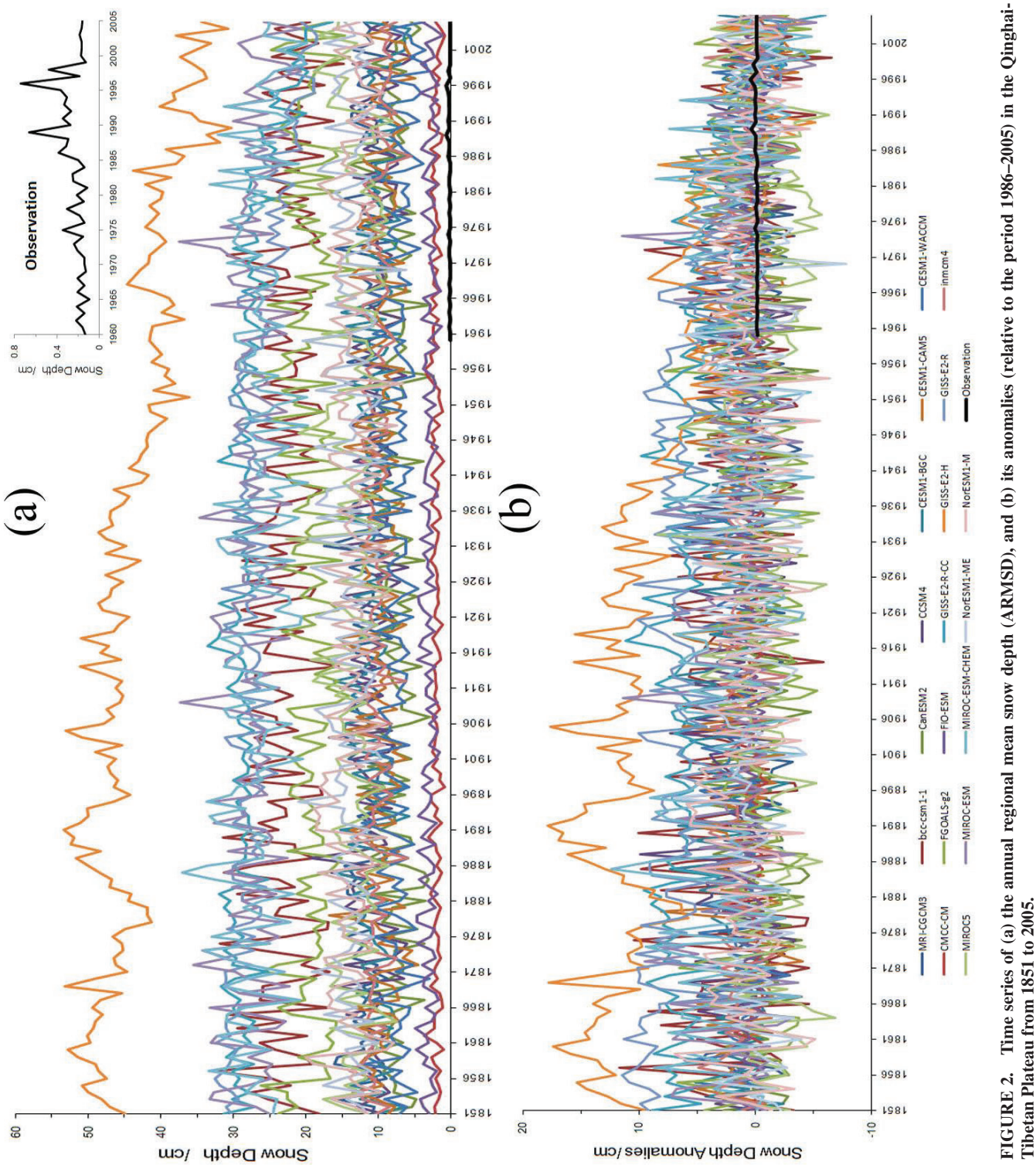


**FIGURE 2. Time series of (a) the annual regional mean snow depth (ARMSD), and (b) its anomalies (relative to the period 1986–2005) in the Qinghai-Tibetan Plateau from 1851 to 2005.**

the Middle Qinghai-Tibetan Plateau. Almost all of the model simulations show the maximum regions for the standard deviation are the same as the ones for AMSD. The results modeled by CESM1-WACCM and inmcm4 are relatively close to the observations. Figure 5 displays the Taylor diagrams that show the correlations and the standard deviations of the modeled versus the observed AMSD in the Qinghai-Tibetan Plateau. The standard deviation values simulated by FIO-ESM, CMCC-CM, and CESM1-WACCM are relatively small, but the mean AMSD values simulated by these models are much larger than those of the PMSR observation. The spatial correlation values between the modeled and the observed AMSD are relatively big for MRI-CGCM3, CCSM4, and CESM1-BGC.

### *TEMPORAL VARIATION OF THE SIMULATED SNOW FROM 1960 TO 2005*

The variation of the observed ARMSD is computed using the daily snow depths from the 72 weather stations from 1960 to

**TABLE 2**

**Trends and correlation coefficients for the observation and simulations.**

| Model number | Model name | TR1 ($cma^{-1}$) | TR2 ($cma^{-1}$) | R1 | R2 | R3 | R4 |
|---|---|---|---|---|---|---|---|
| 1 | bcc-csm1-1 | –0.0160 | –0.0575 | 0.27 | 0.44 | –0.07 | –0.37 |
| 2 | CanESM2 | 0.0034 | –0.0026 | 0.58 | 0.44 | –0.04 | 0.07 |
| 3 | CCSM4 | –0.0125 | –0.0149 | 0.72 | 0.39 | 0.06 | 0.40** |
| 4 | CESM1-BGC | –0.0114 | –0.0611 | 0.71 | 0.37 | 0.15 | –0.13 |
| 5 | CESM1-CAM5 | –0.0054 | –0.0374 | 0.66 | 0.43 | 0.04 | –0.18 |
| 6 | CESM1-WACCM | –0.0081 | –0.0646 | 0.66 | 0.44 | –0.10 | –0.33 |
| 7 | CMCC-CM | 0.0006 | –0.0128 | 0.64 | 0.34 | –0.04 | –0.08 |
| 8 | FGOALS-g2 | 0.0018 | 0.0018 | 0.28 | 0.37 | 0.05 | 0.21 |
| 9 | FIO-ESM | –0.0033 | 0.0021 | 0.31 | 0.31 | –0.18 | –0.10 |
| 10 | GISS-E2-H | –0.0917 | –0.1793 | 0.58 | 0.43 | –0.33 | –0.65 |
| 11 | GISS-E2-R | –0.0533 | –0.1696 | 0.40 | 0.26 | –0.32 | –0.59 |
| 12 | GISS-E2-R-CC | –0.0388 | –0.1960 | 0.39 | 0.23 | –0.22 | –0.46 |
| 13 | inmcm4 | –0.0091 | –0.0255 | 0.59 | 0.69 | –0.15 | –0.41 |
| 14 | MIROC-ESM | –0.0093 | –0.0563 | 0.32 | 0.45 | –0.21 | –0.34 |
| 15 | MIROC-ESM-CHEM | –0.0188 | –0.0880 | 0.33 | 0.51 | 0.14 | –0.13 |
| 16 | MIROC5 | –0.0026 | 0.0903 | 0.44 | 0.38 | 0.04 | 0.29* |
| 17 | MRI-CGCM3 | –0.0065 | 0.0088 | 0.76 | 0.42 | 0.09 | 0.24 |
| 18 | NorESM1-M | –0.0045 | –0.0485 | 0.57 | 0.41 | –0.35 | –0.72 |
| 19 | NorESM1-ME | –0.0010 | 0.0040 | 0.55 | 0.40 | –0.15 | 0.13 |
| | Observation | — | 0.0031 | 1.00 | 1.00 | 1.00 | 1.00 |

TR1 = trend of ARMSD from 1851 to 2005.
TR2 = trend of ARMSD from 1960 to 2005.
R1 and R2 = respective spatial correlation coefficients for the AMSDs and standard deviations of AMSD between the simulations and the PMSR observation.
R3 and R4 = respective temporal correlation coefficients for the ARMSDs and the 5-year-smoothing ARMSDs between the simulations and the station observation.
Positive correlation coefficient values marked by * and ** pass, respectively, the test of the 90% and 95% confidence level.

2005 (see in Fig. 6). The variations of the simulated ARMSD by the 19 models in the same period in the Qinghai-Tibetan Plateau are also shown in Figure 6. From 1960 to 2005, the ARMSDs show decreasing trends for most of the models but increasing trends for the observation. The trend coefficients (TR2) of ARMSDs are listed in Table 2. Only five models display positive trends that agree with the observation. The temporal correlation coefficients (see R3 in Table 2) between the observation and the simulated ARMSDs are positive for seven models and do not pass the level-of-significance test.

The maximum values of the observed ARMSD and its 5-year-smoothing values both occur at 1996 (Fig. 6). The snow is obviously decreasing from 1996 to 2005. So, 1996 is regarded as the inflection point of snow depth trend. The snow appears as an increasing trend from 1960 to 1996 and as a decreasing trend from 1996 to 2005, according to the observations from 72 stations in Qinghai-Tibetan Plateau. This result agrees with the previous research results (Wei et al., 2002; Gao et al., 2003; Zhang et al., 2008; Wang et al., 2009; Ma et al., 2011).

The inter-decade correlations, indicated by the temporal correlation coefficients (see R4 in Table 2) between the 5-year-smoothing sets of the observation and the simulated ARMSDs, are better than the inter-annual correlation (R3). The CCSM4 results pass the 95% confidence level, the MIROC5 results pass the 90% confidence level, and the MRI-CGCM3 and FGOALS-g2 results come close to passing the 90% confidence level. The 5th polynomial fit of the snow depth for 46 years long may show the characteristics of inter-decadal variation of the snow in addition to the trend. The 5th polynomial fits of snow depths (Fig. 6) show that the inter-decadal variations of the ARMSD of these four models are mainly consistent to one of the observation.

### *21ST-CENTURY CHANGES IN THE SNOW CLIMATE IN THE TIBETAN PLATEAU*

In the last section, the simulated snow characteristics are analyzed and compared with the observations in the Qinghai-Tibetan Plateau. The results show the snow depth is simulated poorly by most CMIP5 models at present. Nonetheless, certain relatively good models must be selected to project future snow changes. The seven indices are set using the analysis of the Results section in this paper: (1) a maximum ARMSD occurs in the late 1990s; (2) the snow decreases in the early 21st century; (3) the trend of the ARMSD (see TR2 in Table 2) is increasing from 1960 to 2005; (4) the inter-annual correlation coefficient (see R3

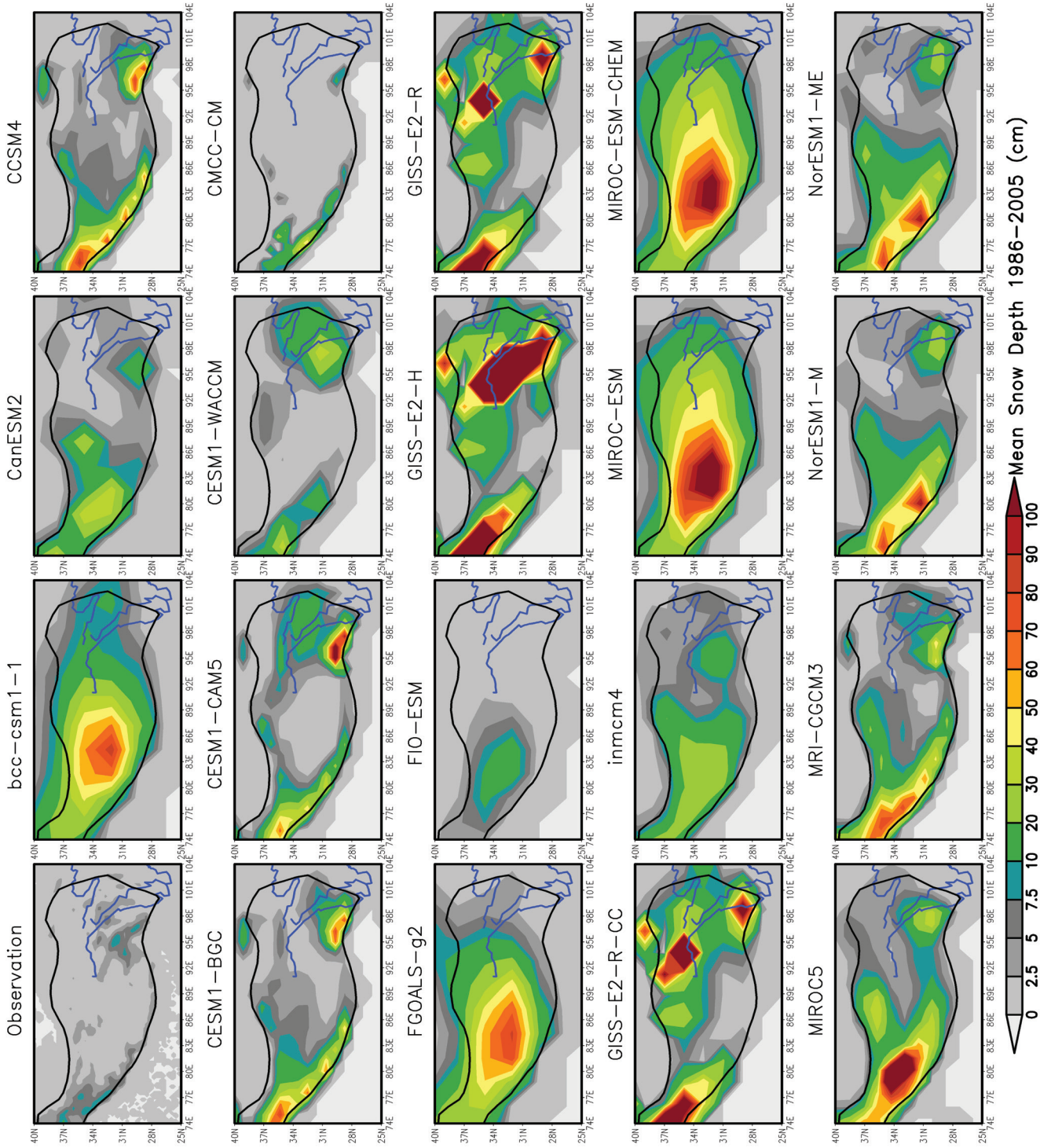


**FIGURE 3. Geographical distributions of the annual mean snow depth (AMSD) for the passive microwave satellite remote-sensing (PMSR) observation and 19 CMIP5 models simulation during the period from 1986 to 2005 in the Qinghai-Tibetan Plateau. The black curve shows the outline of the Plateau above the 3000 m sea level. The blue curves indicate the Yellow River and the Yangzi River.**

in Table 2) between the simulated and the observed ARMSD is relatively large from 1960 to 2005; (5) the inter-decade correlation coefficient (see R4 in Table 2) between the simulated and the observation ARMSD is relatively large from 1960 to 2005; (6) the spatial correlation coefficient (see R1 in Table 2) between the simulated and the observed AMSD is relatively large from 1986 to 2005; and (7) the spatial correlation coefficient (see R2 in Table 2) between the simulated and the observed standard deviation of AMSD is relatively large from 1986 to 2005. According to these indices, the MIROC5, MRI-CGCM3, and FGOALS-g2 models are selected as relatively good models for modeling the plateau snow. CCSM4 has a negative trend (–0.0149 cm $a^{-1}$) and

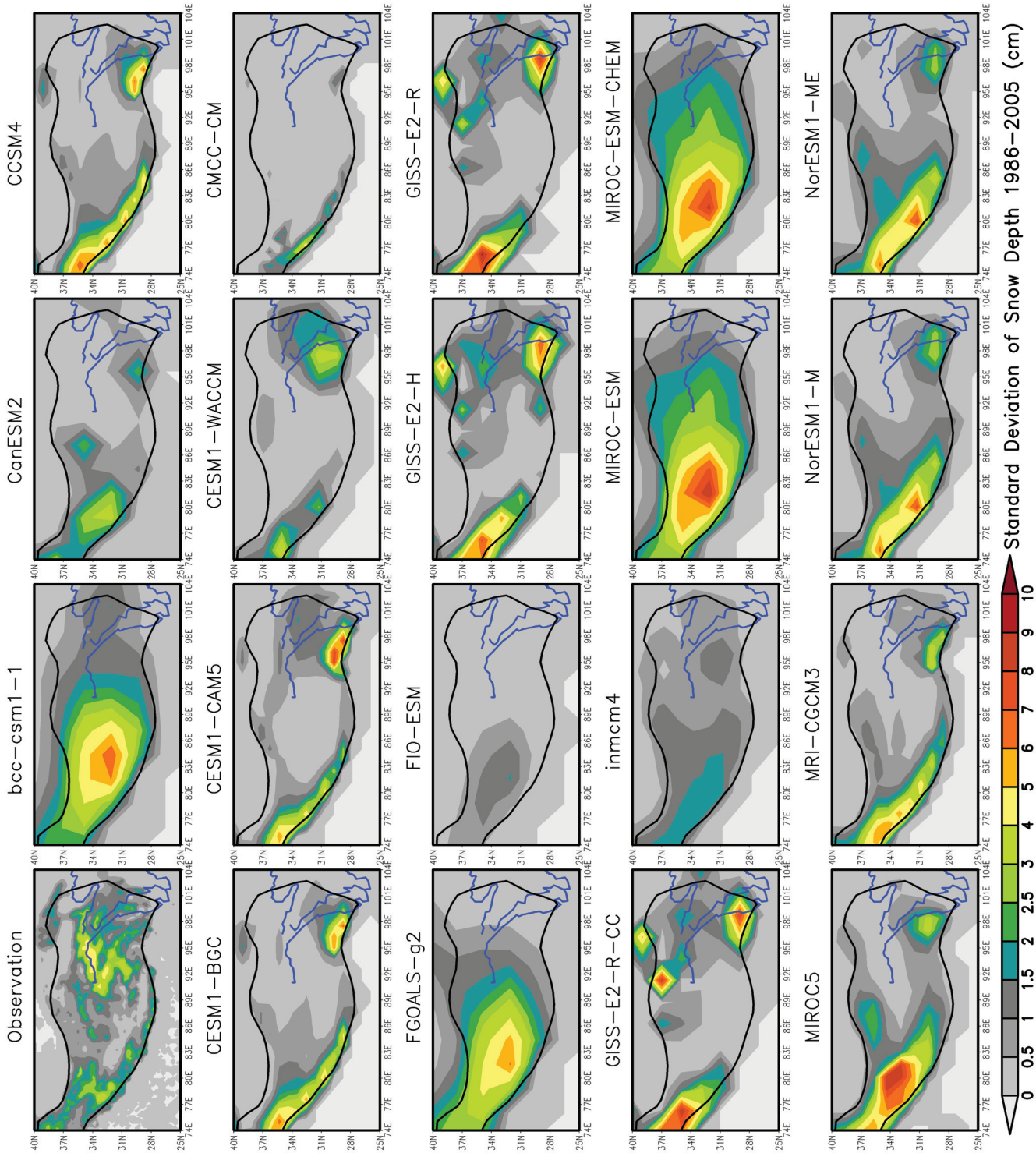


**FIGURE 4. Same as Figure 3 but for the standard deviation of the AMSD.**

can't meet the third index, but it meets the other six indices. The other models can't meet any six among seven indices. Hence, CSCM4 is still selected as a relatively good model for modeling the plateau snow. We will project the 21st century changes of the snow climate in the Qinghai-Tibetan Plateau using these four models in this section.

At first, the ensemble average of these four models is compared to the observation. Figure 7 shows the variations of the standardized ARMSD and their 5-year-smoothing values of the observation and the average of these four CMIP5 models from 1960 to 2005 in the Qinghai-Tibetan Plateau. The variations are most consistent for the 5-year-smoothing but little

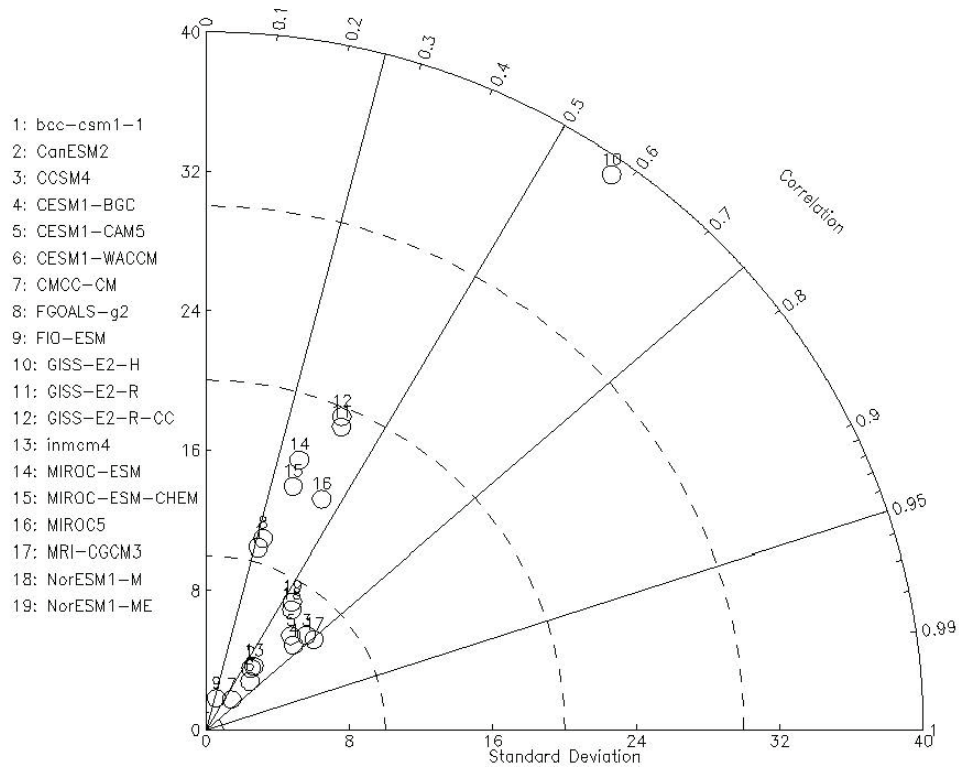


**FIGURE 5. Taylor diagrams showing the correlations and the standard deviations of the modeled versus the observed AMSD in the Qinghai-Tibetan Plateau. The radial coordinates display the modeled versus the observed correlation coefficient, and the *x*-axis displays the normalized standard deviation (the modeled standard deviation divided by the measured standard deviation). A model that perfectly matches the observations would reside at point (1, 1). The model numbers in Table 1 are shown on the circles, and the model names are displayed at the left side of the figure.**

consistent for the inter-annual ARMSDs between the average simulations and the observations. The inter-annual correlation coefficient between the observation and the ensemble average ARMSD is 0.11. This value is larger than the one of any single model (see R3 in Table 2). But it only passes the 75% confidence level. The inter-decadal correlation coefficient for the 5-year-smoothing ARMSDs between the observations and the ensemble average simulations is 0.57. This value is larger than the one of any single model (see R4 in Table 2) and passes the 99% confidence level. The result of the ensemble average is better than any single model when comparing with observations in the periods from 1960 to 2005. We may project the trend and inter-decadal variation by the ensemble average of these four models.

Figure 8 shows the variations of the modeled ARMSD from 2007 to 2099 using the four models under different RCPs in the Qinghai-Tibetan Plateau. The snows simulated by the four models all decrease from the present to the late 21st century in the Qinghai-Tibetan Plateau. The changes in the ARMSD display little differences under RCP2.6 in contrast with those of RCP4.5. The trend coefficients of the ARMSD under RCP2.6, RCP4.5, and RCP8.5 are approximately –0.06, –0.06, and –0.07 cm $a^{-1}$, respectively. The snows simulated by MIROC54 and FGOALS-g2 change more dramatically. The changes of the ARMSD also produce smaller differences under RCP2.6 than RCP4.5. The trend coefficients of the ARMSD under RCP2.6, RCP4.5, and RCP8.5 are approximately –0.11, –0.11, and –0.16 cm $a^{-1}$, respectively.

The changes of the mean ARMSD simulated by the four models under different RCPs are also shown in Figure 8. The snow decreases from 2007 to 2999 in the Qinghai-Tibetan Plateau, and the mean trend coefficients of the ARMSD under RCP2.6, RCP4.5, and RCP8.5 are approximately –0.08, –0.08, and –0.11 cm $a^{-1}$, respectively. The snow changes in stages. Figure 9 shows the accumulative anomaly curves of the mean ARMSD simulated by the four models under different RCPs. The maximum values of the accumulative anomalies under RCP2.6, RCP4.5, and RCP8.5 occur respectively in 2037, 2042, and 2053, which indicates the inflection points of snow depth changes. The snow depths will decrease more obviously from 2037, 2042, and 2053 under RCP2.6, RCP4.5, and RCP8.5, respectively. The trends decrease gently under RCP2.6 and RCP4.5 but more obviously under RCP8.5.

## Conclusions

From 1851 to 2005, the ARMSDs show decreasing trends for most of the models but slight increasing trends for CMCC-CM, FGOALS-g2, and CanESM2; the simulated ARMSD anomalies vary from –10 cm to 20 cm, and the amplitudes exhibit obvious decreases over the most recent 50 years in the Qinghai-Tibetan Plateau.

According to the PMSR observation, two maximum snow regions exist in the Qinghai-Tibetan Plateau. One region reaches from the Har goolun Range in the West Plateau to the Himalayan Mountains in the South Plateau, and the other ranges from the Nyainqentanggula Range to the East Tanggula Range and the Bayan har Range in the East Plateau. These two maximum snow regions are well simulated by most models. The spatial distributions of the mean simulated AMSD from MRI-CGCM3, CCSM4, CESM1-BGC, CESM1-CAM5, and CESM1-WACCM are quite similar to the PMSR observation. The maximum AMSD values simulated by all 19 models are 5–15 times that

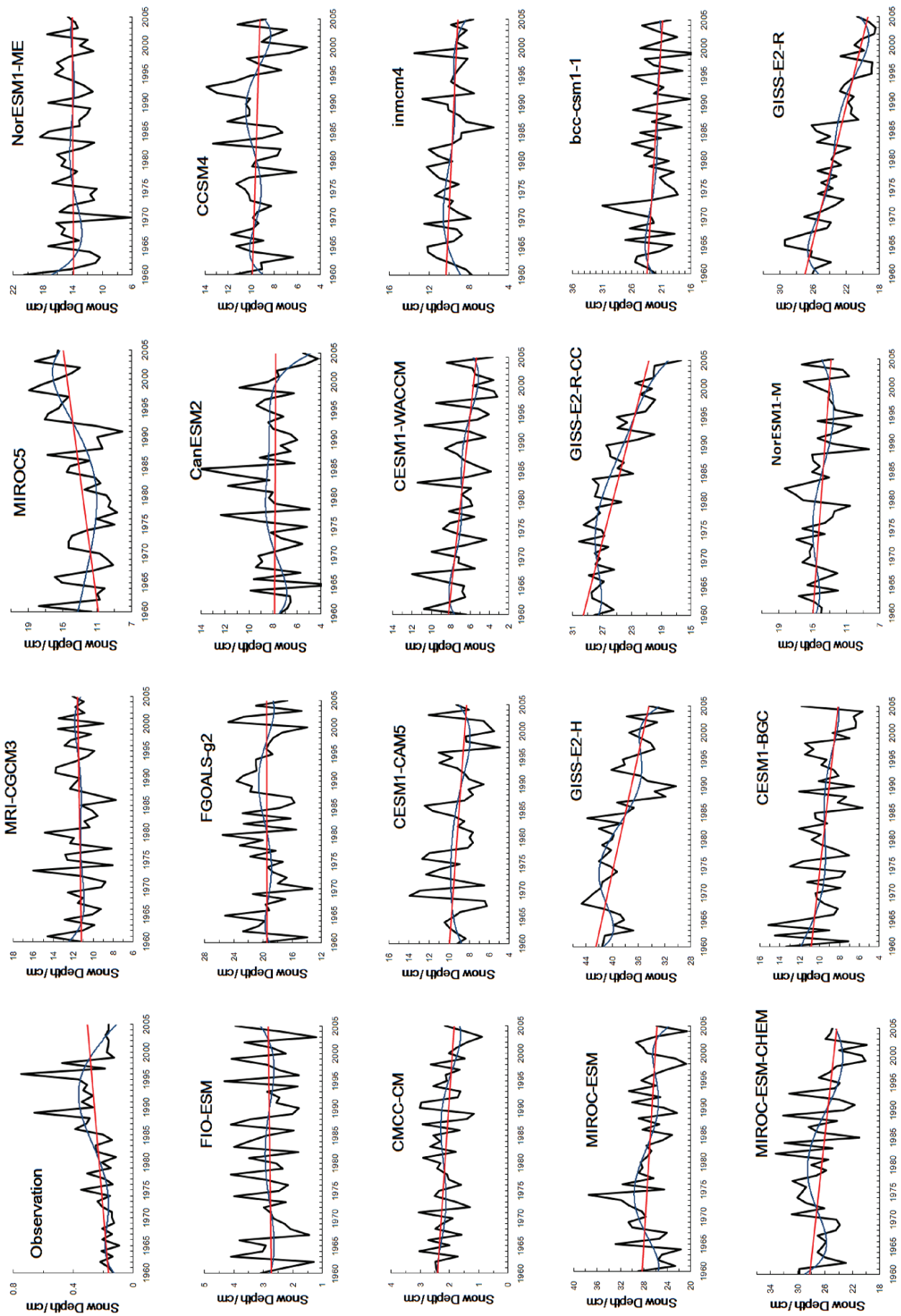


**FIGURE 6. Variations of the ARMSD (black curves) from 1960 to 2005 in the Qinghai-Tibetan Plateau. The red lines indicate the trends. The blue curves show the 5th polynomial fits.**

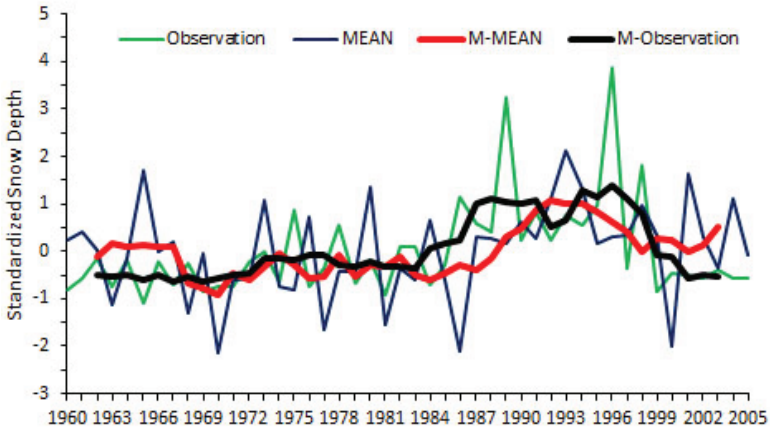


**FIGURE 7. Variations of the standardized ARMSD from 1960 to 2005 in the Qinghai-Tibetan Plateau. The green line and the black line indicate the observation and its 5-year-smoothing Value (M-observation), respectively. The blue line and the red line indicate the averaged value (MEAN) of the 4 CMIP5 models and its 5-year-smoothing Value (M-MEAN), respectively.**

of the one observed by SMMR. The standard deviation values simulated by FIO-ESM, CMCC-CM, and CESM1-WACCM are relatively small, but the simulated mean AMSD values are much larger than that of the PMSR observation. According to the PMSR observation, the inter-annual snow variation occurs primarily in the Middle and East Tibetan Plateau. Almost all of the 19 simulated results produce the same maximum regions for the AMSD and its standard deviation. The results modeled by inmcm4 are relatively close to that of the observation.

According to the observations from 72 stations, the snow depth has an increasing trend from 1960 to 1996 and a decreasing trend from 1996 to 2005. Decreasing ARMSDs are simulated by most of the models but show increases in the observations from 1960 to 2005. Only five models have positive trends that agree with the observation. The inter-decade correlations are better than the inter-annual correlations. The models that produce relatively good simulations of the temporal variations of the plateau snow from 1960 to 2005 are CCSM4, MIROC5, MRI-CGCM3, FGOALS-g2, CanESM2, and NorESM1-ME.

According to certain indices, CCSM4, MIROC5, MRI-CGCM3, and FGOALS-g2 are selected only as relatively good models for modeling the plateau snow. The 21st-century changes in the snow climate in the Qinghai-Tibetan Plateau are projected simply using these four models, and the simulations predict decreasing snow from the present to the late 21st century in the Qinghai-Tibetan Plateau. The snow shows decreasing trends from 2007 to 2999 in the Qinghai-Tibetan Plateau, and the mean trend coefficients of the ARMSD under RCP2.6, RCP4.5, and RCP8.5 are approximately –0.08, –0.08, and –0.11 cm $a^{-1}$, respectively. The snow changes in stages; the trends are insignificant from 2010 to 2030 and decreasing from 2030 to 2065 under three RCP models. The trends decrease slightly under RCP2.6 and RCP4.5 but more sharply under RCP8.5 from 2065 to 2099. The snow depths will decrease more obviously from 2037, 2042, and 2053 under RCP2.6, RCP4.5, and RCP8.5, respectively. The trends decrease gently under RCP2.6 and RCP4.5, but more obviously under RCP8.5.

## Discussion

The projection of snow is a very complicated scientific problem. To obtain accurate results, snow parameterization needs to be improved by the assessment of simulated snow, some factors related to snow such as temperature and precipitation need to be simulated very well, and the estimating methods based on an ensemble of GCMs need to be investigated. In this paper, the projection is achieved simply.

The causes of the apparent strong overestimation of snow depths of the Qinghai-Tibetan Plateau from CMIP5 models are complicated. Su et al. (2013) evaluated precipitation and temperature over the eastern Tibetan Plateau by comparing the outputs of 24 CMIP5 GCMs with ground observations for the period 1961–2005. The results suggest that the majority of the models have cold temperature biases and positive precipitation biases. The cold temperature biases and the positive precipitation biases both contribute to excessive simulated snow depths over the Qinghai-Tibetan Plateau. The precipitation bias in winter when the snow falls might be even larger than the annual mean precipitation bias. A possible difference between GCMs in altitude of each grid mesh and the corresponding observation points might also be responsible for a part of the cold bias of the models. Indeed observations are generally done in the valleys, that is, at altitudes that may be lower than those of the corresponding grid point. The simulated snow depths are also impacted by other factors such as the snow schemes in land surface process models and the simulated the midlatitude atmospheric circulation of each model. In this paper, we only evaluate the ability of CMIP5 models to model the depth of Qinghai-Tibetan Plateau snow in past decades, in order to identify systematic model biases and models that agree best with observations. The causes of overestimation of snow depths will be analyzed to improve the CMIP5 GCMs later.

It can be seen from our analysis that the snow depth values are simulated poorly by most CMIP5 models at present. All 19 models have the apparent strong overestimation of snow depth values in the Qinghai-Tibetan Plateau and need be improved by analyzing the causes. Some models, such as MRI-CGCM3, CCSM4, CESM1-BGC, CESM1-CAM5, and CESM1-WACCM, have good simulation to the spatial distributions of the mean AMSD. But only inmcm4 has relatively close simulation to the spatial distributions of the standard deviation of AMSD. Some other models, such as CCSM4, MIROC5, MRI-CGCM3, FGOALS-g2, CanESM2, and NorESM1-ME, produce relatively good simulations of the temporal variations of the plateau snow from 1960 to 2005. The good models to simulate different characteristics of snow depth are not the same. In this paper, only

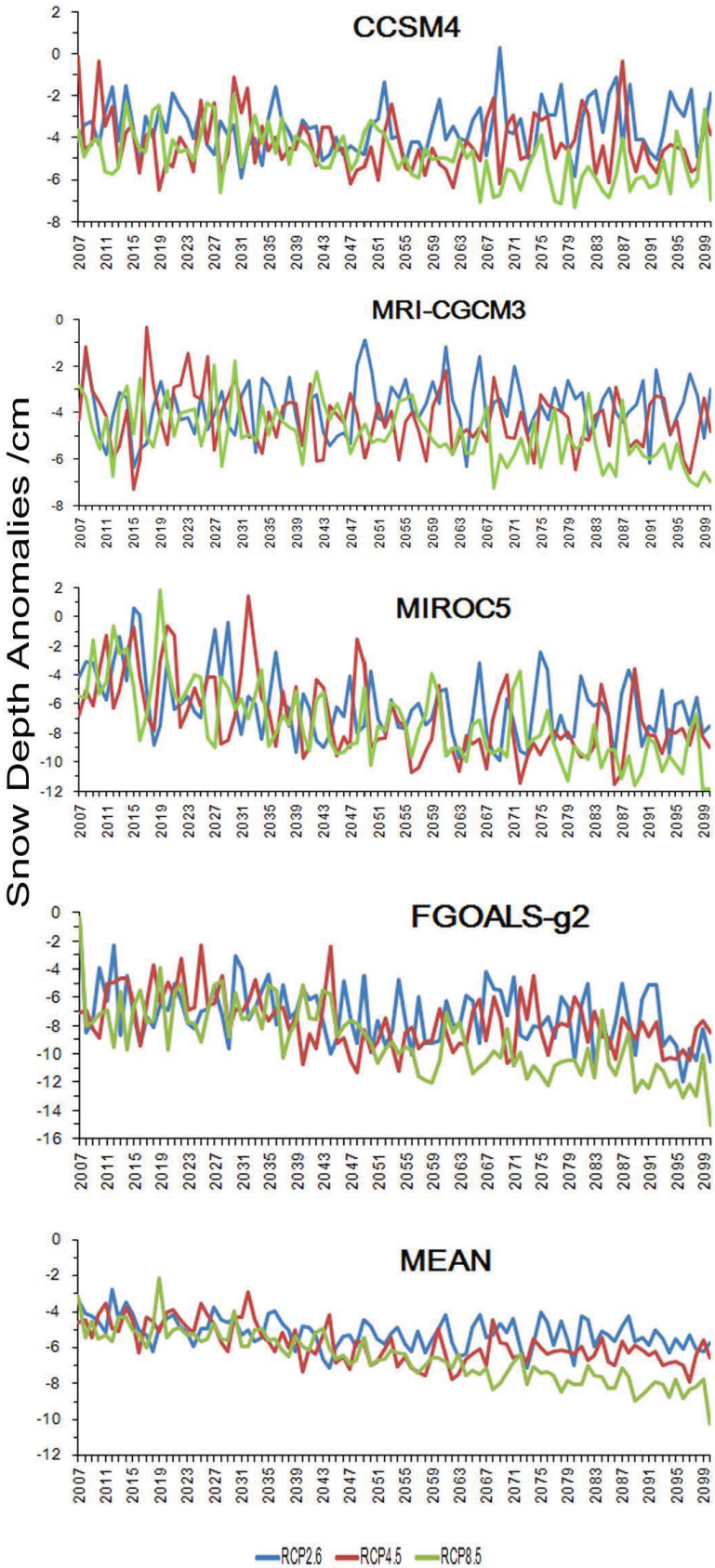


**FIGURE 8. Variations of the modeled ARMSD from 2007 to 2099 under different representative concentration pathways (RCPs) in the Qinghai-Tibetan Plateau.**

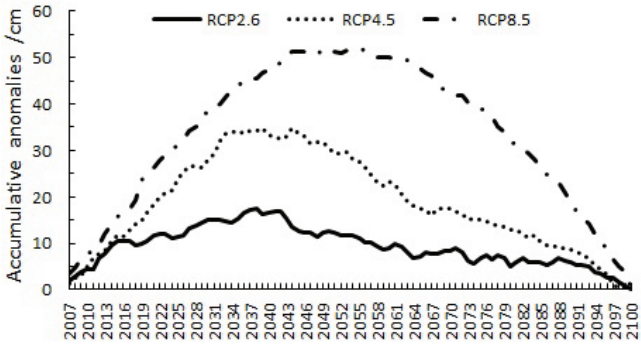


**FIGURE 9. The accumulative anomaly curves of the mean ARMSD simulated by the four models under different RCPs.**

simulated levels are assessed for 19 CMIP5 models. We hope that the causes to overestimate and underestimate the characteristics of snow can be researched so that the models can be better improved by scientists.

## Acknowledgments

We express gratitude to the anonymous reviewers for their constructive comments and suggestions. This study was supported by National Natural Science Foundation of China (Grant No. 41330527), Fund for Creative Research Groups of National Natural Science Foundation of China (No. 41321001), and the Global Change Research Program of China (2014CB953903).

## References Cited

Blanford, H. F., 1884: On the connection of the Himalayan snowfall with dry winds and seasons of drought in India. *Proceedings of the Royal Society of London,* 37: 3–22.

Brown, R. D., and Mote, P. W., 2009: The response of northern hemisphere snow cover to a changing climate. *Journal of Climate*, 22: 2124–2145, http://dx.doi.org/10.1175/2008JCLI2665.1.

Brown, R. D., and Robinson, D. A., 2011: Northern hemisphere spring snow cover variability and change over 1922–2010 including an assessment of uncertainty. *The Cryosphere*, 5: 219–229, http://dx.doi.org/10.5194/tc-5-219-2011.

Brutel-Vuilmet, C., Ménégoz, M., and Krinner, G., 2013: An analysis of present and future seasonal northern hemisphere land snow cover simulated by CMIP5 coupled climate models. *The Cryosphere*, 7: 67–80, doi http://dx.doi.org/10.5194/tc-7-67-2013.

Chang, A.T.C., Foster, J. L., and Hall, D. K., 1987: Nimbus-7 SMMR derived global snow cover parameters. *Annals of Glaciology*, 9: 39–44.

Che, T., Li, X., Jin, R., Armstrong, R., and Zhang, T. J., 2008: Snow depth derived from passive microwave remote-sensing data in China. *Annals of Glaciology*, 49: 145–154.

Chen, X. F., and Song, W. L., 2000: Analysis and application of the relation between the snow in Tibetan Plateau and in Europe and Asia and the summer precipitation in China. *Plateau Meteorology*, 19(2): 215–223.

Clark, M. P., and Serreze, M. C., 2000: Effects of variations in east Asian snow cover on modulating atmospheric circulation over the North Pacific Ocean. *Journal of Climate*, 13: 3700–3710.

Derksen, C., Misurak, K., LeDrew, E., Piwowar, J., and Goodison, B., 1997: Relationship between snow cover and atmospheric circulation, central North America, winter 1988. *Annals of Glaciology*, 25: 347–352.

Frei, A., and Gong, G., 2005: Decadal to century scale trends in North American snow extent in coupled atmosphere-ocean general circulation models. *Geophysical Research Letters*, 32: L18502, doi http://dx.doi.org/10.1029/2005GL023394.

Gao, R., Wei, Z. G., Dong, W. J., and Wang, C. H., 2003: Variation of the snow and frozen soil over Qinghai-Xizang Plateau in the late twentieth century and their relations to climatic change. *Plateau Meteorology*, 22(2): 191–196.

Gregory, J. M., and David, M. W., 2010: Long-term variability in northern hemisphere snow cover and associations with warmer winters. *Climatic Change*, 99: 141–153, doi http://dx.doi.org/10.1007/s10584-009-9675-2.

Groisman, P. Y., Karl, T. R., and Heim, R. R., 1993: Influences of the North American snowfall and snow cover with recent global temperature changes. *NOAA Glaciological Data Report*, GD-25: 44–51.

Guo, Q. Y., and Wang, J. Q., 1986: Winter-spring snows over the Qinghai-Tibetan Plateau and its influence on East Asia monsoon. *Plateau Meteorology*, 5(2): 116–124.

Han, F., Zhang, B., Yao, Y., Zhu, Y., and Pang, Y., 2011: Mass elevation effect and its contribution to the altitude of snow line in the Tibetan Plateau and surrounding areas. *Arctic, Antarctic, and Alpine Research*, 43(2): 207–212, http://dx.doi.org/10.1657/1938-4246-43.2.207.

Immerzeel, W. W., Pellicciotti, F., and Bierkens, M. F. P., 2013: Rising river flows throughout the twenty-first century in two Himalayan glacierized watersheds. *Nature Geoscience*, 6: 737–741, http://dx.doi.org/10.1038/NGEO1896.

Ji, Z. M., and Kang, S. C., 2013: Projection of snow cover changes over China under RCP scenarios. *Climate Dynamics*, 41: 589–600, http://dx.doi.org/10.1007/s00382-012-1473-2.

Kang, S. C., Xu, Y. W., You, Q. L., Flügel, W. A., Pepin, N., and Yao, T. D., 2010: Review of climate and cryospheric change in the Tibetan Plateau. *Environmental Research Letters*, 5: 015101, http://dx.doi.org/10.1088/1748-9326/5/1/015101.

Li, P. J., 1995: Distribution of snow cover in the High Asia. *Journal of Glaciology and Geocryology*, 17(4): 291–198.

Ma, L. J., Qin, D. H., Bian, L. G., Xiao, C. D., and Luo, Y., 2011: Assessment of snow cover vulnerability over the Qinghai-Tibetan Plateau. *Advances in Climate Change Research*, 2(2): 93–100, http://dx.doi.org/10.3724/SP.J.1248.2011.00093.

Moore, G. W. K., 2012: Surface pressure record of Tibetan Plateau warming since the 1870s. *Quarterly Journal of the Royal Meteorological Society*, 138: 1999–2008, http://dx.doi.org/10.1002/qj.1948.

Moore, G. W. K., 2013: Tibetan ice core evidence for an intensification of the East Asian jet stream since the 1870s. *Atmospheric Science Letters*, 14: 235–242, http://dx.doi.org/10.1002/asl2.445.

Peacock, S., 2012: Projected twenty-first-century changes in temperature, precipitation, and snow cover over North America in CCSM4. *Journal of Climate*, 25: 4409–4425, http://dx.doi.org/10.1175/JCLI-D-11-00214.1.

Qian, Y. F., Zheng, Y. Q., Zhang, Y., and Miao, M. Q., 2003: Responses of China's summer monsoon climate to snow anomaly over the Tibetan Plateau. *International Journal of Climatology*, 23: 593–613, http://dx.doi.org/10.1002/joc.901.

Qin, D., and Xiao, C., 2009: Global climate change and cryospheric evolution in China. *European Physical Journal Conferences*, 1: 19–28, http://dx.doi.org/10.1140/epjconf/e2009-00907-x.

Qin, D. H., Liu, S. Y., and Li, P. J., 2006: Snow cover distribution, variability and response to climate change in Western China. *Journal of Climate*, 19: 1820–1833, http://dx.doi.org/10.1175/JCLI3694.1.

Räisänen, J., 2007: Warmer climate: less or more snow? *Climate Dynamics*, 30: 307–319, http://dx.doi.org/10.1007/s00382-007-0289-y.

Räisänen, J., and Eklund, J., 2012: 21st century changes in snow climate in Northern Europe: a high-resolution view from ENSEMBLES regional climate models. *Climate Dynamics*, 38: 2575–2591, http://dx.doi.org/10.1007/s00382-011-1076-3.

Stephen, J. D., and Ross, D. B., 2007: Recent northern hemisphere snow cover extent trends and implications for the snow-albedo

feedback. *Geophysical Research Letters*, 34: L22504, http://dx.doi.org/10.1029/2007GL031474.

Stocker, T. F., Qin, D., Plattner, G. K., Tignor, M., Allen, S. K., Boschung, J., Nauels, A., Xia, Y., Bex, V., and Midgley, P. M. (eds.), 2013: *Climate Change 2013: The Physical Science Basis. Contribution of Working Group I to the Fifth Assessment Report of the Intergovernmental Panel on Climate Change.* Cambridge, U.K., and New York: Cambridge University Press, 317–361.

Su, F. G., Duan, X. L., Chen, D. L., Hao, Z. C., and Cui, L., 2013: Evaluation of the global climate models in the CMIP5 over the Tibetan Plateau. *Journal of Climate*, 26: 3187–3208, http://dx.doi.org/10.1175/JCLI-D-12-00321.1.

Taylor, K. E., Stouffer, R. J., and Meehl, G. A., 2012: An overview of CMIP5 and the experiment design. *Bulletin of the American Meteorological Society*, 93: 485–498, http://dx.doi.org/10.1175/BAMS-D-11-00094.1, 2012.

Wang, C. H., Wang, Z. L., and Cui, Y., 2009: Spatial distributions and interannual variations of snow cover over China in the last 40 years. *Sciences in Cold and Arid Regions*, 1(6): 0509–0518.

Wang, Z. L., Wang, X. P., and Li, Y. H., 2013: Analyses of snow cover based on passive microwave remote sensing data and observed data over the Tibetan Plateau. *Journal of Glaciology and Geocryology,* 35(4): 783–792.

Wei, Z. G, and Lu, S. H., 1995: Distribution of snow cover on the Qinghai-Xizang Plateau and its influence on surface albedo. *Plateau Meteorology*, 14(2): 67–73.

Wei, Z. G., Luo, S. W., Dong, W. J., and Li, P. J., 1998: Snow cover data on Qinghai-Xizang Plateau and its correlation with summer rainfall in China. *Quarterly Journal of Applied Meteorology*, 9(supplement): 39–46.

Wei, Z. G., Huang, R. H., Chen, W., and Dong, W. J., 2002: Spatial distributions and interdecadal variations of the snow at the Tibetan Plateau weather stations. *Chinese Journal of Atmospheric Sciences*, 26(4): 346–358.

You, Q. L., Kang, S. C., Ren, G. Y., Fraedrich, K., Repin, N., Yan, Y. P., and Ma, L. J., 2011: Changes of snow depth and number of snow day in the eastern and central Tibetan Plateau from observational data. *Climate Research*, 46: 171–183, http://dx.doi.org/10.3354/cr00985, 2011.

Zhang, J. H., Wu, Y., and Yao, F. M., 2008: Study on the snow distribution and influencing factors in Northern Tibet based on remote sensing information. *Chinese Journal of Geophysics*, 51(4): 1013–1021.

Zhang, J., Song, Y., Li, Z. C., and Zhao, P., 2012: Interdecadal change of snow depth in winter over the Tibetan Plateau and its effect on summer precipitation in China. *Sciences in Cold and Arid Regions*, 4(1): 0046–0055, http://dx.doi.org/10.3724/SP.J.1226.2012.00046.

Zhu, X., and Dong, W. J., 2013: Evaluation and projection of northern hemisphere March-April snow covered area simulated by CMIP5 coupled climate models. *Advances in Climate Change Research*, 9(3): 173–234, http://dx.doi.org/10.3969/j.issn.1673-1719.2013.03.003.

*MS accepted May 2015*